Observational Technological Innovations and Future Development of the Lijiang Coronagraph

Xuefei Zhang , Yu Liu * , Tengfei Song , Mingyu Zhao , Xiaobo Li , Mingzhe Sun , Feiyang Sha , Xiande Liu

Posted Date: 18 February 2026

doi: 10.20944/preprints202602.1308.v1

Keywords: coronagraph; dual-band observation; stray light suppression; coronal heating; coronal mass ejection (CME)

Article

Observational Technological Innovations and Future Development of the Lijiang Coronagraph

Xuefei Zhang [1,2], Yu Liu [3,*], Tengfei Song [1,2], Mingyu Zhao [1,2], Xiaobo Li [1], Mingzhe Sun [4], Feiyang Sha [3] and Xiande Liu [5]

[1] Yunnan Observatories, Chinese Academy of Sciences, Kunming 650216, China
[2] Yunnan Key Laboratory of Solar Physics and Space Science, Kunming 650216, China
[3] College of Physical Science and Technology, Southwest Jiaotong University, Chengdu 611756, China
[4] Shandong Provincial Key Laboratory of Optical Astronomy and Solar-Terrestrial Environment, Institute of Space Sciences, Shandong University, Weihai 264209, China
[5] School of Physics and Astronomy, Yunnan University, Kunming 650504, China
* Correspondence: lyu@swjtu.edu.cn

Abstract

As a core ground-based coronal observation facility in the low-latitude and high-altitude regions of China, the Lijiang Coronagraph takes advantage of the natural endowments of the Lijiang Astronomical Observation Station, such as an altitude of 3200 meters and low atmospheric turbulence. It has gone through a complete development process from introduction through China-Japanese cooperation to independent innovation and iteration. This paper systematically summarizes the core technological innovation achievements of this facility, including the upgrade of the automatic operating system, the integration of the dual-band observation system, the stray light suppression technology based on the image difference method before and after cleaning, as well as the high-precision image calibration and registration technology. These innovations have significantly improved observation efficiency and data quality, laying a solid foundation for high-quality observations. At the scientific research level, the observation data reveal that $1.1R_0$ (solar radius) is a highly correlated region between coronal green line brightness and magnetic field intensity. It also confirms a strong correlation between the coronal green line and the SDO/AIA 211Å extreme ultraviolet band (correlation coefficient: 0.89 - 0.99), which can support the research on early warning of Coronal Mass Ejections (CMEs). These achievements provide key data support for the verification of coronal heating mechanisms and the exploration of the origin of the slow solar wind. The technical experience accumulated by the Lijiang Coronagraph has not only laid a solid foundation for the research and development of China's next-generation large-aperture coronagraphs, but also promoted China's leapfrog development from being a follower to a parallel runner in the international field of low coronal observation, making it an important part of the global coronal observation network.

Keywords: coronagraph; dual-band observation; stray light suppression; coronal heating; coronal mass ejection (CME)

1. Introduction

The corona, as the outermost layer of the solar atmosphere, its plasma dynamic evolution process is closely related to major frontier issues in solar physics, such as coronal heating mechanisms, solar wind origin, CMEs. It is a core research object for revealing the laws of solar activities and space weather effects [1–4]. Since the brightness of the corona is only one millionth of that of the solar photosphere, conventional observations are severely interfered by strong light. Ground-based coronagraphs, through artificial solar eclipse technology, have broken through the natural limitation of short-term observations during total solar eclipses and become the core supporting equipment for regular coronal observations [5–7]. High-altitude regions have unique advantages such as weak

 doi:10.20944/preprints202602.1308.v1

atmospheric turbulence, low background brightness, and a large number of sunny days per year, making them the preferred areas for the construction of ground-based coronagraphs. They provide natural observation conditions for capturing fine coronal structures and weak radiation signals [8,9].

The Lijiang Astronomical Observation Station in Yunnan (altitude: 3200m, longitude: 100°2′ E, latitude: 26°42′ N) has become the primary site for low-latitude and high-altitude coronal observation in China due to its excellent observation environment. The Yunnan Observatory Coronal Green Line Imaging System (YOGIS) is developed from the Nagoya University Green Line Imaging System (NOGIS) of the National Astronomical Observatory of Japan. It was relocated to the Lijiang Astronomical Observation Station through international cooperation and renamed for use in 2013 [5,10]. As China's first ground-based internally occulted coronagraph put into regular operation, its completion has filled the gap in the field of continuous low-latitude coronal observation in China [11]. However, the design parameters of the NOGIS were optimized for its original observational environment and scientific objectives. After its relocation to Lijiang, the instrument is confronted not only with challenges posed by the high-altitude, low-pressure conditions, the updated scientific objectives, and the upgrade of the integrated system, but also with the demand for high-time-resolution observations of solar eruptive events during the solar activity maximum. Its original observational environment, detector performance, and operating system are no longer sufficient to meet the coronagraph's requirements for high signal-to-noise ratio, high resolution, and integrated multi-device observations [12].

To this end, we have carried out systematic technical upgrades and multi-channel observation system integration for the YOGIS, with the central objectives of adapting it to the extreme high-altitude observational environment in Lijiang, improving its temporal resolution, and enhancing the instrument's autonomous observation capability. This paper focuses on elaborating the key technological breakthroughs of YOGIS in the optimization of the core optical system, the iteration of detection devices, the innovation of observation modes, and the construction of dual-band observation channels. It also systematically analyzes the performance improvement of the upgraded instrument in detecting fine coronal structures and capturing dynamic characteristics of plasma. These research achievements not only provide high-quality observation data support for the study of basic scientific issues such as coronal heating mechanisms and solar wind origin, but also offer reusable technical paradigms and engineering practice bases for the independent research and development as well as multi-band upgrade and transformation of subsequent ground-based coronagraphs in China. They are of great strategic significance for promoting China's low coronal observation to leap from following the international pace to keeping pace with it.

2. Development History and Technical Orientation of Lijiang Coronal Observation

Since 2010, the coronagraph team of Yunnan Observatories has launched a large-scale site selection project. It has conducted systematic monitoring for more than two years in over 60 candidate regions including Xinjiang, Tibet, and Yunnan, and finally selected two high-quality observation sites, namely Lijiang in Yunnan and Daocheng in Sichuan [13]. In 2013, we successfully built a green line coronagraph at the Lijiang Astronomical Observation Station and obtained clear coronal green line images for the first time. This has strongly confirmed the great potential of the high-altitude regions in western China in the field of coronal observation and laid a solid foundation for subsequent technological research and development (Figure 1).

 doi:10.20944/preprints202602.1308.v1

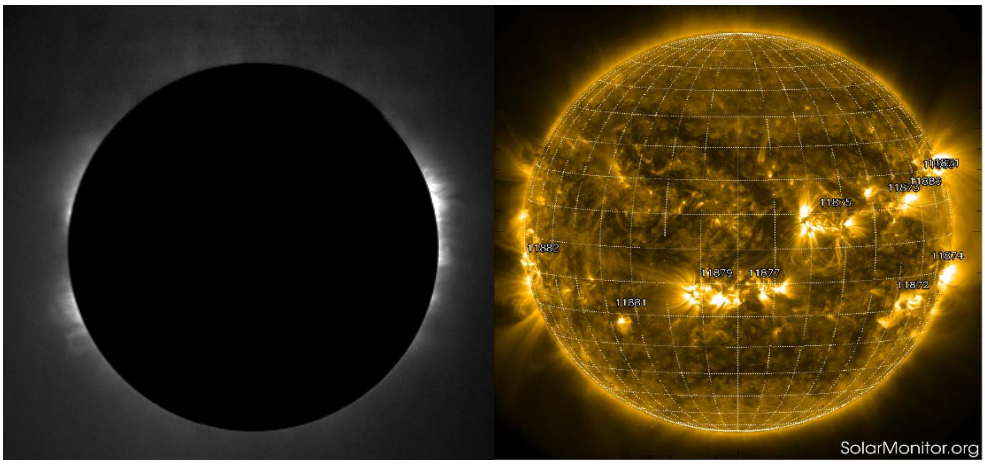

Figure 1. On 25 October 2023, the YOGIS successfully acquired its first coronal images. **Light:** visible-band data obtained by the Lijiang coronagraph; **Right:** extreme ultraviolet (EUV) band data from the Solar Dynamics Observatory (SDO) [14].

The development history of Lijiang coronal observation is a history of continuous exploration and constant breakthroughs in technological iteration. Since the establishment of the China-Japanese cooperative coronal observation station in 2013, the equipment has undergone three generations of technological upgrades, and its observation capability has achieved leapfrog improvement. In 2017, the team, in cooperation with the University of Science and Technology of China, built a high-altitude experimental base for coronagraphs in Lijiang (Figure 2). In 2018, a prototype coronagraph developed under the leadership of Shandong University with the in-depth participation of this team successfully obtained coronal green line data at this base, achieving a series of key technological breakthroughs in coronagraph development. The site construction and ground experiments during this period have accumulated a large amount of valuable measured data for core technologies such as the environmental adaptability optimization and stray light suppression of balloon-borne coronagraphs.

Figure 2. Light: Commemorative photo of the completion of the YOGIS international cooperation station. **Right:** Location 1 indicates the original construction site of YOGIS; Location 2 denotes the high-altitude test base for the coronagraph; Location 3 marks the site of the Lijiang 2.4-meter optical telescope . The image is sourced from Google Earth.

Relying on a sub-project of the Strategic Priority Research Program (Class A) "Honghu Project" of the Chinese Academy of Sciences, Yunnan Observatories, together with multiple scientific research institutions, launched the research and development of a balloon-borne white-light coronagraph. It successfully overcame key technical bottlenecks such as the suppression of stray light at the million-

 doi:10.20944/preprints202602.1308.v1

level and developed a 50 mm-aperture white-light coronagraph [15]. On February 27, 2021, this instrument completed ground observations at Wuming Mountain in Daocheng, Sichuan, with an altitude of nearly 4800 meters. It obtained the first white-light coronal images through China's independently developed white-light coronagraph, fully verifying the ground observation performance of the equipment. On October 4, 2022, with the help of the high-altitude balloon platform of the Aerospace Information Research Institute of the Chinese Academy of Sciences, the coronagraph was sent to the stratosphere at an altitude of 30 kilometers in Da Qaidam, Haixi Prefecture, Qinghai [16]. It successfully carried out continuous observations for 5 hours and obtained nearly 20,000 white-light coronal photos. This is the first time in the international solar physics community that white-light observations of the inner corona have been carried out at this altitude, demonstrating that our team has the capability to independently carry out balloon-borne astronomical observations and obtain key data[17,18].

With the continuous progress of technology, Lijiang coronal observation has ushered in a landmark upgrade. The Spectroscopic Imaging Coronagraph for Meridian Project Phase II (SICG), as China's first independently developed ground-based coronagraph put into regular operation, passed the process test and obtained the first batch of coronal observation images in October 2023, filling the relevant gaps in the field of coronagraph development in China. The equipment adopts an advanced optical system and detector, realizing the leap from monochromatic imaging to multi-band spectroscopic observation, and can accurately obtain key physical parameters such as coronal temperature, density, and velocity. In terms of observation bands, SICG has unique advantages in observing the Fe X 6374 Å (low-temperature corona) and Fe XIV 5303 Å (high-temperature corona) spectral lines. The Fe X 6374 Å spectral line can be used to study the magnetohydrodynamic coupling process and material transport phenomena in the low-temperature corona, while the Fe XIV 5303 Å spectral line can help explore the heating mechanism and energy release process in the high-temperature corona. The collaborative observation of these two spectral lines provides powerful technical support for a comprehensive analysis of coronal physical processes, and also enables Lijiang coronal observation to occupy an important position in the international coronal observation network, becoming a key node for studying the magnetohydrodynamic coupling process of the low corona.

3. Observational Technological Innovations: From Noise Suppression to Precision Calibration

3.1. Reconstruction of the Observation Platform

As China's first ground-based coronagraph put into regular observation, YOGIS officially began its construction in 2013. The initial observation site was selected with significant scientific consideration, located 1 km outside the Lijiang Astronomical Observation Station compound — a location that was once a core candidate site for monitoring the Lijiang Astronomical Observatory's foundation [19]. During the initial observation phase, a dedicated observation platform was already built at this site. The platform featured a circular structure with a diameter of 4.5 meters, erected approximately 12 meters above the ground, effectively mitigating the interference of near-surface atmospheric turbulence on observations. Notably, this initial platform was not equipped with a dome facility commonly used in astronomical observations, yet the optical components of the coronagraph are extremely sensitive to environmental factors such as humidity and rain. Therefore, in the early stages of YOGIS's operation, customized rainproof equipment was specifically installed. This setup not only protected the instrument from rain and snow erosion but also minimized the obstruction of the observation field of view caused by the equipment itself (Figure 3).

 doi:10.20944/preprints202602.1308.v1

Figure 3. Light: In the early stages of YOGIS construction in 2013, the coronagraph lacked rainproof facilities. A movable rain shelter was installed on the roof of the circular building. The image shows staff members opening the roof shelter via pulleys to conduct observations. **Right:** In 2014, a dome was designed and installed according to the dimensions of the circular building, upgrading the equipment for safeguarding the observation environment.

To further enhance observation stability and data quality, the new YOGIS observation platform was officially completed and put into operation in 2017, relying on multi-party technical collaboration and joint research efforts. The core breakthrough of the new platform lies in its pier design, with its natural frequency successfully increased to over 12 Hz. This key indicator far exceeds the requirements for regular observations, effectively resisting external disturbances such as wind forces and ground vibrations, and thus providing a solid structural guarantee for the high-precision tracking observation of coronal activities. Meanwhile, the supporting high-altitude test site for the coronagraph was completed simultaneously. This test site not only provides an exclusive experimental space for YOGIS equipment upgrades and parameter optimization, but also establishes a domestic R&D and verification platform for key coronagraph technologies, laying an important practical foundation for the development of subsequent independently-developed coronal observation instruments in China (Figure 4).

Figure 4. Light: YOGIS operates on the newly constructed platform, ensuring the regular coronal monitoring capability of the coronagraph. **Right:** This is the high-altitude coronagraph test base, dedicated to conducting ground-based coronagraph testing and experimental research; China's independently developed regular-operation coronagraph underwent its trials right here.

 doi:10.20944/preprints202602.1308.v1

3.2. Intelligent Upgrading of the Observation Control System

During the initial construction phase of YOGIS, constrained by technical conditions, the supporting graphical user interface (GUI) had relatively simple functions, only capable of displaying basic observation data, with core operational procedures highly dependent on manual intervention. Specifically, equipment controls such as dome rotation and the start/stop of observation instruments had to be manually performed on-site. Monitoring of critical environmental parameters, including atmospheric humidity, temperature, and wind speed, also relied on manual recording and judgment.

To address this issue, we introduced the Astronomy Common Object Model (ASCOM) - Alpaca open-source standardized astronomical control platform to reconstruct and upgrade the observation control system [12,20]. Through systematic integration, the three core systems of YOGIS — the telescope system responsible for target acquisition, the pointing and tracking system ensuring observation precision, and the auxiliary system covering environmental monitoring and equipment power supply—were organically integrated, enabling collaborative linkage and centralized management of each subsystem. Meanwhile, based on the actual needs of scientific research and operation and maintenance (O&M), three differentiated observation modes were innovatively designed: the Standard Observation Mode, suitable for regular scientific observation tasks, which can automatically complete the entire observation process according to preset parameters; the Rapid Observation Mode, targeting sudden solar events such as CMEs, which can quickly activate the equipment and focus on the observation target; and the Engineering Debugging Mode, which provides a dedicated interface for technicians to calibrate equipment parameters and troubleshoot faults, balancing research efficiency with O&M convenience.

Figure 5 illustrates the user interface of the coronagraph operation control system before and after the upgrade. This intelligent control system demonstrated exceptional operational performance during four years of field observation validation from 2021 to 2024: the overall system availability reached 92%, with the proportion of effective operational time far exceeding the industry average; the Mean Time Between Failures (MTBF) reached approximately 1100 hours, significantly reducing equipment maintenance frequency and costs; more critically, the observation time utilization rate increased from 65% to 90%, completely resolving the past issue of wasted observation windows caused by delays in manual operations.

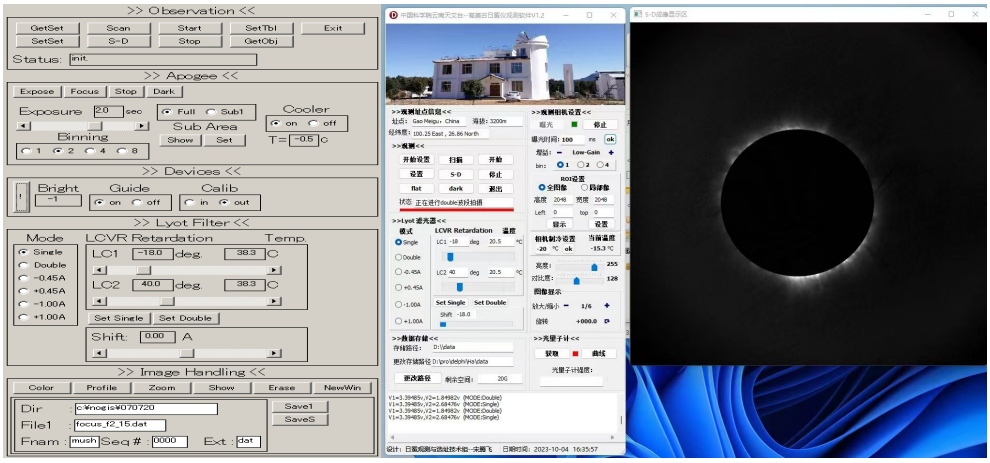

Figure 5. The upgraded operation control system not only enables the control of the coronagraph data acquisition terminal but also adds controls for the equatorial mount's pointing and tracking functions. Additionally, it incorporates real-time wavelength display for the birefringent filter, coronal image visualization, and status monitoring for the dome and weather conditions.

3.3. Construction of a Multi-Channel Observation System

In terms of inheriting and optimizing the core optical system, YOGIS fully retained the 100 mm effective aperture objective lens from the original NOGIS. This objective lens has a focal length of

 doi:10.20944/preprints202602.1308.v1

1490 mm at 5300 Å (corresponding to the core band of the coronal green line). Its optical parameters, which have been verified through long-term practice, can accurately focus the faint light of the corona, making it a core component for ensuring basic observation accuracy. To address the critical issue of stray light interference during local observations, we conducted a special shading optimization of the telescope tube interior, covering the entire inner wall with a customized, matte black special coating. This coating exhibits high absorption and low reflectivity properties, enabling efficient absorption of stray reflected light inside the tube and fundamentally reducing the interference of non-target light on observation signals, thereby laying a solid optical foundation for subsequent acquisition of high signal-to-noise ratio (SNR) data.

The initial YOGIS system was equipped with a 1024 × 1024 pixel CCD detector, paired with a traditional mechanical shutter. Although this shutter configuration is a classic setup for early astronomical observation equipment, its limitations have become increasingly apparent when combined with the specific requirements of high-altitude coronal observations in Lijiang: the minute mechanical vibrations generated by the shutter blade movement can cause image blurring and loss of detail; metal transmission components are susceptible to low temperatures, leading to jamming, delays, or even failure to open/close properly. To this end, we comprehensively replaced it with a high-performance, cooled CMOS detector with 2048 × 2048 pixels. Compared to traditional CCDs, the cooled CMOS not only quadruples the pixel count but also significantly enhances the detail capture capability of the observation field of view.

To overcome the limitations of single-band observations and expand the dimensions of coronal research, we tackled the core technical challenges of dual-band observations and successfully added a coronal red line observation channel. Figure 6 illustrates the optical design for multi-channel observations with YOGIS, where the red region represents the measurement terminal for the coronal red line. By employing optical path dispersion compensation technology, we accurately corrected the optical path deviations when switching between the green and red line bands, ensuring the spatial alignment accuracy of dual-band observations. Simultaneously, through the collaborative optimization of the detection and control systems, we achieved alternating observations between the two bands. A typical observation sequence can complete continuous switching from green line single peak → red line single peak → green line double peak → red line double peak, ensuring both observation continuity and avoiding time loss caused by band switching. This image displays the quasi-simultaneous observation results of the coronal green line and red line(Figure 7). In the left panel (Fe XIV 5303 Å , green-line observation), bright emission regions are concentrated at discrete solar limb locations (e.g., the right and lower-left sectors), tracing the accumulation of high-temperature plasma ($T \approx 2 \times 10^6$ K) — a feature consistent with active-region coronal streamers or precursor structures of CMEs. By contrast, the right panel (Fe X 6374 Å , red-line observation) exhibits distinct bright-region extents and intensity profiles relative to the green line (e.g., enhanced red-line emission in the left sector), revealing that the spatial distribution of medium-low temperature plasma ($T \approx 1 \times 10^6$ K) is not spatially coincident with that of the high-temperature component. The central composite panel resolves the spatial overlap of the two spectral bands: mixed red-green emission regions denote the coexistence of 1×10^6 K and 2×10^6 K plasma at the same location, while single-color dominated regions correspond to plasma regimes governed by a single temperature component.

 doi:10.20944/preprints202602.1308.v1

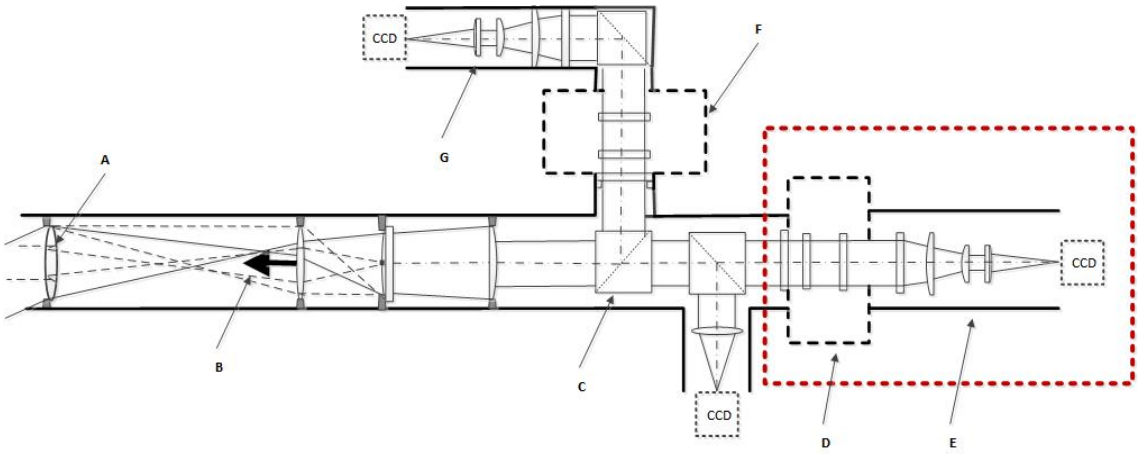

Figure 6. As shown in the figure, this is the optical design layout of the YOGIS dual-channel observation mode. Here, A: Objective lens; B: Inner occulter; C: Polarizing beam splitter; D: 6374 Å Lyot filter; E: Relay lens imaging system; F: 5303 Å Lyot filter; G: Relay lens imaging system.

Such dual-band observations constitute foundational data for probing coronal heating mechanisms and coronal streamer dynamics. For example, regions of concentrated green-line emission typically align with locales of steep magnetic field gradients (sites of active magnetic reconnection or wave-driven heating), whereas the red-line emission morphology encodes the density and temperature gradient profiles of the coronal plasma. These panels are not merely visual renderings of coronal morphology; they represent critical observational constraints for characterizing temperature distributions and plasma dynamics in the low corona (1.03 – 2.0 $R_{\odot}$). Their core utility lies in disentangling the multi-temperature hierarchical structure of the corona via the contrast and superposition of the two spectral band signals.

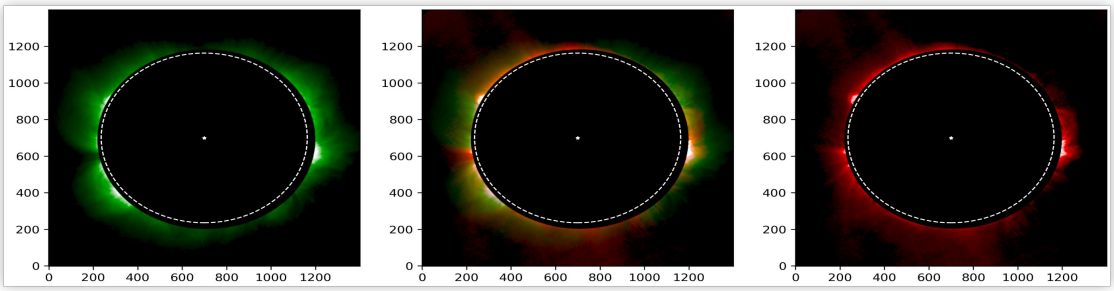

Figure 7. As shown in the figure, this is the optical design layout of the YOGIS dual-channel observation mode. Here, A: Objective lens; B: Inner occulter; C: Polarizing beam splitter; D: 6374 Å Lyot filter; E: Relay lens imaging system; F: 5303 Å Lyot filter; G: Relay lens imaging system.

3.4. Breakthroughs in Stray Light Suppression Technology

Using the YOGIS as a test platform, we innovatively constructed a dedicated mirror dust imaging optical path, enabling precise and visual detection of dust particles on the objective lens surface. This ingenious optical path design leverages the existing optical structure of the observation system to establish a dual-mode operational mechanism of "forward observation - backward imaging":

- In the normal coronal observation mode, the solar corona, acting as an object at infinity, is precisely imaged onto the inner occulter disk at the focal plane after refraction by the 100 mm effective aperture objective lens. The occulter disk blocks the intense light from the photosphere, allowing only the faint coronal light to enter the subsequent optical system.
- In the dust detection mode, a newly added collimator creates a folded optical path, altering the direction of light propagation. This transformation effectively makes the objective lens itself, which originally served as the "imaging lens," the object of observation. Scattered light emanating

 doi:10.20944/preprints202602.1308.v1

from dust particles adhering to the objective lens surface is collimated into parallel light by the collimator. This parallel light is then fully received and imaged by the original imaging components of the coronagraph.

This design represents an essentially reverse and creative application of the objective lens - imaging system paradigm, while fully preserving the original stray light suppression structures within the instrument, such as the non-reflective internal coatings and multi-stage light-blocking apertures. It achieves dust detection while effectively avoiding the strong light interference caused by direct solar illumination, allowing for the inspection of the objective lens cleanliness without the need for instrument disassembly. Through this specialized optical path modification, we successfully captured panoramic images of the dust distribution on the YOGIS objective lens surface, accurately identifying high-scattering risk areas. This lays a solid physical foundation for the precise correction and calibration of stray light in subsequent coronal observation data. Figure 8 shows the optical layout of the coronagraph in dust detection mode.

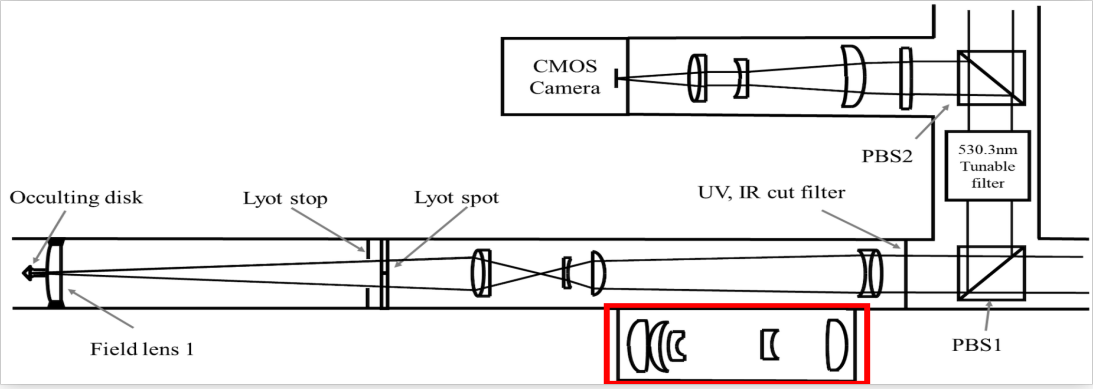

Figure 8. Optical layout of the coronagraph in "dust detection mode" (the red box indicates the relay lens group for dust imaging). The system realizes reverse observation of the objective lens surface by reusing the original coronal observation optical path, enabling visualization of dust particles on the objective lens.

Building upon this optical path detection capability, we conducted systematic research on the quantitative subtraction of dust scattering backgrounds and proposed an innovative and practical image differencing method before and after cleaning [21]. This method uses the observation image of the objective lens in a clean state as a reference and performs a pixel-level differencing operation with the image obtained when dust is present. This process accurately isolates the pure background signal from dust scattering, leading to the first establishment of a radial attenuation model for the dust scattering background in coronagraphs. Analysis and validation using YOGIS observation data revealed significant and regular characteristics in dust scattering intensity: the scattering intensity exhibits a strictly linear attenuation trend with increasing heliocentric distance (in solar radii). Furthermore, the attenuation coefficient is positively correlated with the total dust intensity on the objective lens surface—the greater the amount of dust, the higher the attenuation coefficient, and the broader the range of scattering influence. As shown in Figure 9, this is the captured dust image of the coronagraph's objective lens.

Based on this core discovery, we further introduced feature point matching technology. By extracting the gray-scale distribution and spatial location features of the dust scattering background, we constructed an adaptive background subtraction algorithm, enabling the precise removal of dust scattering noise from the original coronal images. This technical solution has been thoroughly validated through actual YOGIS observations. After its application, the SNR of the coronal images was improved by an additional 30%, completely eliminating the interference from dust stray light. This provides reliable data support for subsequent scientific analyses, including the intensity calibration of coronal green and red lines, Doppler velocity measurements, and the dynamic evolution analysis of

 doi:10.20944/preprints202602.1308.v1

coronal plasma. Concurrently, this comprehensive solution, encompassing both optical path design and algorithmic modeling, offers a novel technical approach for ground-based internally-occulted coronagraphs worldwide to address the challenge of dust scattering.

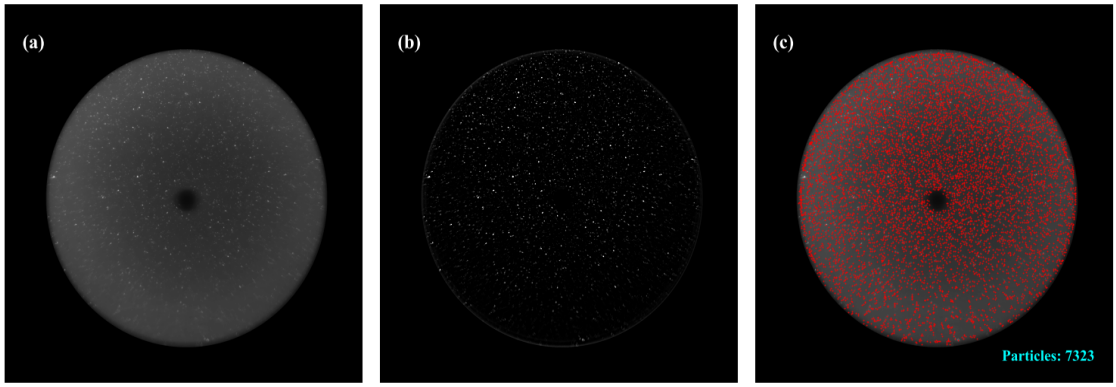

Figure 9. The captured dust images of the coronagraph objective lens surface, from left to right, are described as follows: The first image is the dust map of the objective lens surface: the small black dot corresponds to the "inner occulter disk" (used for blocking intense light), while the tiny bright spots in the background represent dust particles adhering to the objective lens surface. The second image shows all potential dust signals separated from the original map: dust particles with brightness exceeding the threshold are converted to white bright spots, and the background is converted to black (via binarization processing with a threshold of 2). The third image presents real dust particles filtered out (with noise excluded) via algorithms based on the binarized result: Red spots indicate the identified dust particles, which are used for position calibration and brightness identification.

3.5. High-Precision Image Calibration and Multi-Band Registration Technology

Ground-based coronagraphs observe the low corona by creating an artificial solar eclipse using an occulter disk. However, due to factors such as pointing accuracy and temperature fluctuations, the occulter disk cannot always be precisely aligned with the Sun. Figure 10 shows the variation of the solar center offset with time during a day's observation. Furthermore, the observed images lack clear landmarks such as the solar limb, making it difficult to accurately determine key parameters like helioprojective coordinates and the solar radius. This severely limits the joint analysis of multi-instrument and multi-band data.

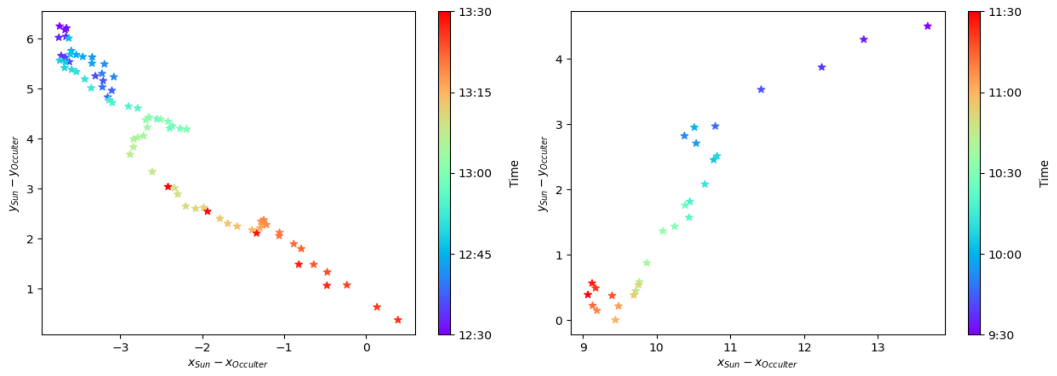

Figure 10. The images show the drift of the solar center relative to the occulter center over observation time during coronal observations (Observation date: 2024 November 11; Unit: pixel). The left and right panels illustrate the horizontal (x-axis) and vertical (y-axis) drift of YOGIS and SICG, respectively. Different colors correspond to the observation times of the day, with relatively small drift values near noon.

The core approach to solving this problem is to use calibrated space-based images with known heliocentric coordinates, solar radius, and north-south pole orientation as a reference. By performing

 doi:10.20944/preprints202602.1308.v1

operations such as translation, rotation, and scaling, the ground-based coronagraph images are registered with these reference images, thereby indirectly obtaining the aforementioned key parameters.

Sha Feiyang et al. proposed an Automated High-Precision Registration Algorithm (APRIL). Using SDO/AIA 211 Å extreme ultraviolet (EUV) images as the reference, APRIL achieves precise registration between ground-based coronal green line images and the reference images [22]. This enables the successful mapping of coronal images onto the Helioprojective Cartesian Coordinate (HCC) system. Under optimal data quality conditions, the registration accuracy is better than $0.1'$, and in most cases, it is no worse than $0.4'$.

This method has been thoroughly validated using observational data from two coronagraphs: the YOGIS and SICG. The validation covers 100 days of data from 2013 to 2024, as well as 34 days of statistical data from 2015 and 2024. These tests confirm its broad applicability, effectively supporting studies of coronal transient activities and joint data analysis across multiple instruments. Additionally, it provides technical support for improving the pointing accuracy of coronagraphs. It should be noted that this method assumes the presence of clear coronal structures around the solar disk and is not suitable for coronal images during solar minimum periods.

4. Data Applications

4.1. Coronal Structure and Activity Observations

The coronal heating mechanism is one of the most challenging core problems in solar physics, and it has long been a research focus for scientists worldwide. The YOGIS with its unique coronal green-line observation capability, provides rich and critical observational data for this field, offering essential support for in-depth analysis of this complex mechanism.

Using the 2D coronal green-line images from theYOGIS, combined with photospheric magnetograms from the SDO/HMI instrument, Zhang et al. [23] calculated the coronal magnetic field strength via the Potential Field Source Surface (PFSS) model and conducted an in-depth correlation analysis between the two datasets. Their study revealed that the correlation coefficient between the green-line intensity and magnetic field strength reaches a maximum of 0.82 at a height of $1.1R_{\odot}$, which corresponds exactly to the apex of closed coronal loops. In terms of loop distribution, the correlation coefficient at the loop apex is consistently above 0.8, while the correlation at the loop footpoints is weaker and exhibits significant fluctuations. Additionally, in extended studies covering the $\pm 40^{\circ}$ latitude range and a complete Carrington rotation (CR 2143, 27 days), the maximum correlation coefficient consistently appears at $1.1R_{\odot}$. This finding clarifies the special role of the $1.1R_{\odot}$ height in coronal physics research: it not only provides key clues for studies on the origin of the slow solar wind (suggesting this height may be a critical source region for the slow solar wind) but also opens new directions for coronal heating mechanism research. The study hypothesizes that closed coronal loop heating is driven by a combination of DC (current dissipation) and AC (Alfvén wave, magnetoacoustic wave dissipation) mechanisms, with DC mechanisms dominating at the loop apex. Furthermore, the established correlation between green-line brightness and magnetic field strength provides a reliable reference for subsequent indirect coronal magnetic field estimation and coronal heating model validation.

To build a bridge for multi-wavelength coronal research, Zhang et al. [24] conducted comparative analyses between green-line data from theYOGIS and EUV band data from the SDO/AIA instrument. They investigated intensity correlations across different coronal regions and structures using two feature extraction algorithms, achieving breakthrough results: the correlation coefficient between the coronal green line and the 211 Å is the highest, ranging from 0.89 to 0.99 (a result not previously reported in the literature), while the correlation coefficient between the green line and the 171 Å is relatively the lowest, ranging from 0.17 to 0.95. This finding strongly supports the connection of physical processes across different coronal heights: ground-based coronal green-line observations and space-based 211 Å observations can complement each other, effectively filling data gaps in green-line observations and laying a solid foundation for long-term studies of the solar activity cycle.

 doi:10.20944/preprints202602.1308.v1

The high correlation coefficient between the coronal green line and the 211Å not only intuitively reflects the physical essence of "unified observation targets" but also carries profound scientific significance and application value. It verifies the consistency of the physical state of inner coronal plasma, builds a complementary bridge between ground-based and space-based observations, and provides a new research tool for core scientific issues such as coronal heating and magnetic field diagnostics. This discovery also points the way for future research—through joint observations of these two bands, the physical processes (e.g., slow solar wind acceleration) at the critical $1.1R_{\odot}$ height can be further revealed, and scientific basis can be provided for the observation scheme design of the next-generation coronagraphs.

4.2. Early Warning of CMEs

Regarding CMEs—a significant solar activity phenomenon—the high time-resolution green-line observations of the YOGIS in fast mode (15 s per frame) can accurately capture their dynamic evolutionary processes. Leveraging its high time-resolution observational capability, the instrument can promptly detect relevant propagation signals when a CME just breaks through the solar surface (at approximately 1.03 $R_{\odot}$). Figure 11 shows taking a bright structure event associated with a C-class flare that occurred on the western limb of the Sun on 2015 January 15 as an example, the corresponding CME was observed by the Large Angle and Spectrometric Coronagraph (LASCO) instrument aboard the Solar and Heliospheric Observatory (SOHO) satellite one hour later [25]. The brightness of this bright structure began to increase at 05:00 (UT) and ceased at 06:30; during the late evolutionary stage, a cusp-shaped structure was clearly observed, with its apex continuously moving outward away from the solar limb(Figure 12). Calculations indicate that the average velocity of the brightest point of the bright structure in the sky plane was approximately 20 kms^{-1}.. Near the brightness peak, the velocity varied from 25 to 15 kms^{-1}. This observational achievement provides a valuable case study for the early identification of CMEs and the calculation of their dynamical parameters, fully demonstrating the crucial role of the YOGIS in the early warning of CMEs.

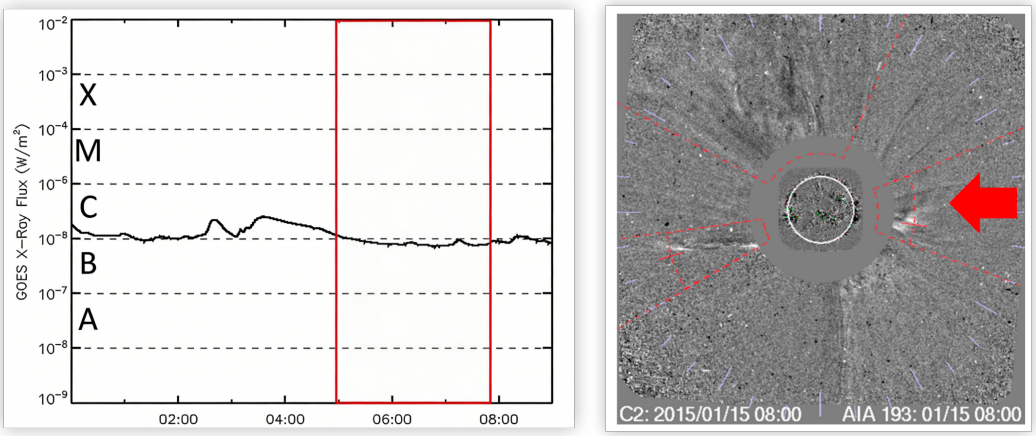

Figure 11. This figure presents the time evolution curve of solar flare soft X-ray flux and its association with CME observations. **Light:** GOES X-ray satellite flux data detected a C-class flare on 15 January 2015. **Right:** The CME observed by LASCO is indicated by the red arrow on the right.

 doi:10.20944/preprints202602.1308.v1

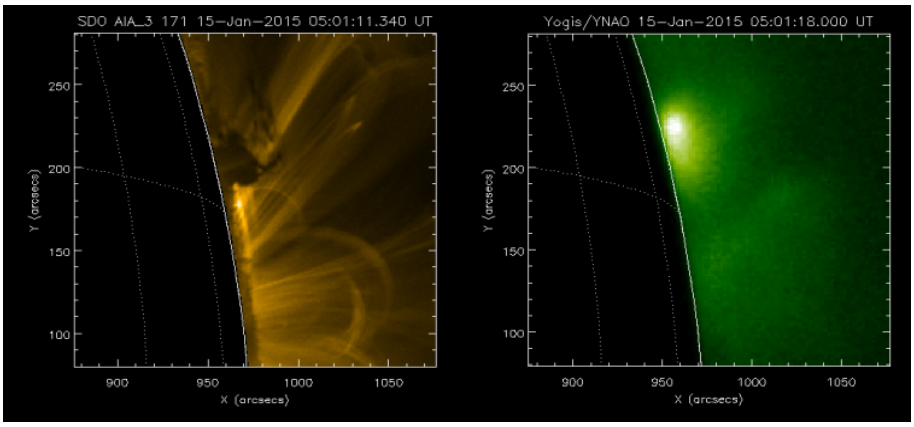

Figure 12. This figure presents the two-dimensional spatial position tracking data of a coronal bright structure in the solar disk coordinate system. Within hours after the C-class flare eruption, bright structures in the corona were observed by SDO/AIA 171 and YOGIS.

5. Future Plans for YOGIS

Despite multiple technical upgrades and significant scientific achievements made with YOGIS, the analysis of fine-scale coronal structures remains severely constrained, limiting its further development and application. Coronal structures encode rich physical information and are key to unraveling the fine-scale physical processes in the corona [26–28]. However, the current spatial resolution of YOGIS is insufficient to resolve these structural details. Overcoming this limitation requires breakthroughs in the fabrication of large-aperture objective lenses. For lenses larger than 500 mm in diameter, critical challenges remain, including the control of material homogeneity and the assurance of ultra-high precision manufacturing. The coronal green line, owing to its high intensity, strong magnetic sensitivity, and its diagnostic potential for high-temperature coronal plasma, makes polarimetric measurement a crucial tool for directly probing coronal magnetic fields. Observational studies have shown that the degree of polarization of the green line depends on the angle between the radial direction and the magnetic field vector [29]. Furthermore, the polarization degree exhibits significant correlations with different coronal structures (e.g., helmet streamers and active regions) and varies systematically with the solar activity cycle, indicating that polarization parameters carry essential information on the physical state of the coronal plasma [30]. Nevertheless, no direct quantitative relationship has yet been established between the spatiotemporal variations of polarization degree/angle and specific plasma flows or turbulence [31]. To address this gap, we plan to upgrade the acquisition terminal of YOGIS by inserting a polarization modulation module — consisting of a rotating waveplate and a static analyzer — downstream of the Lyot birefringent filter. This will enable routine polarimetric measurements, allowing us to study the spatiotemporal evolution of the green line's polarization degree and angle. Such measurements can trace the velocity of coronal plasma flows and detect the onset and propagation of CMEs. Moreover, time-series analysis of the polarization signals will permit the capture of dynamic processes in fine-scale structures such as coronal plumes and jets.

Since its commissioning in 2013, YOGIS has operated under a paradigm of **fixed-interval acquisition followed by post-processing**. The inherent limitations of this scheduled acquisition mode have long remained unresolved. The non-stationary characteristics of stray light, which gradually evolve with the slow degradation of mirror surface contamination, cause systematic day-to-day variations in the signal-to-noise ratio of coronal images. Under the fixed-interval paradigm, data quality at the moment of acquisition is inherently unpredictable. Moreover, the inability to precisely locate the spatial origin of coronal transient events hinders reliable linkage to their source regions on the solar disk. Although coordinate deviations can be partially corrected in post-processing via manual alignment of morphological features, this approach has become an insurmountable bottleneck for tasks requiring real-time transient monitoring and operational space weather forecasting. Drawing on more than a decade of experience in operating and maintaining a high-altitude coronagraph, the

 doi:10.20944/preprints202602.1308.v1

ultimate goal for YOGIS is to achieve unattended, routine coronal observations. This intelligent and autonomous vision comprises four key capabilities:

- Autonomous judgment of observable windows based on real-time measurements of cloud cover and sky background brightness.
- Real-time monitoring of the operating status of critical components, with automatic failover to backup systems or execution of safety procedures upon anomaly detection.
- Event-driven mode switching triggered when specific physical parameters (e.g., total intensity, degree of polarization) extracted from coronal images exceed preset thresholds.
- Automated generation and dissemination of data products to scientific databases.

Realizing such fully intelligent autonomous observations is also a core requirement for establishing coronagraph stations at ultra-high-altitude sites. Higher altitudes offer thinner atmospheres and substantially lower sky-scattered light, providing superior conditions for ground-based coronal diagnostics. However, these advantages come at the cost of severe hypoxia, difficult terrain, and limited accessibility, imposing extreme challenges on observer safety, equipment transportation, and long-term operational expenditure. In the landscape of ground-based coronagraphy, YOGIS is poised to evolve into a new generation of rapid-response, fully automatic coronagraph. Figure 13 illustrates the envisioned fully autonomous observing mode of YOGIS.

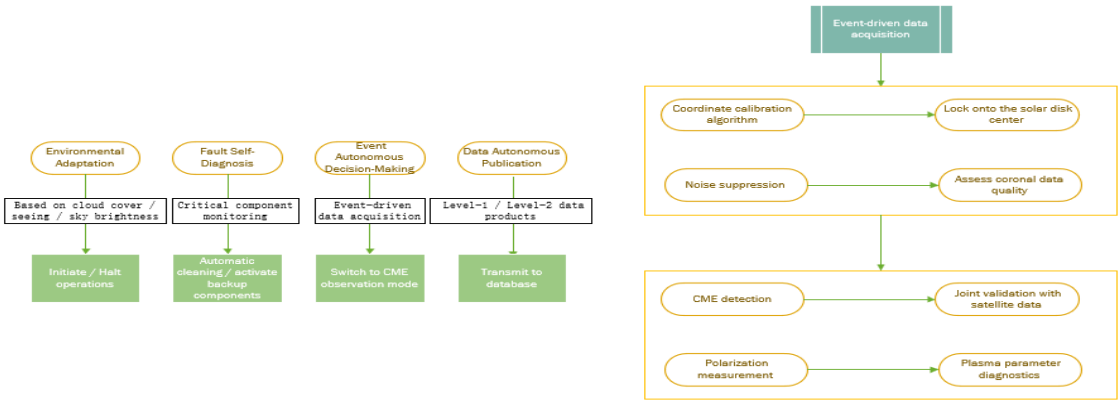

Figure 13. This figure depicts the complete technical architecture of the future fully autonomous observing mode of the YOGIS coronagraph. **Light:** the end-to-end workflow for unattended operation, encompassing autonomous observation condition assessment, equipment status management, event-triggered acquisition of CMEs, and automated data publication. **Right:** the detection pipeline for CME eruptions, ranging from identification of the solar disk center coordinates and coronal image noise suppression to polarimetric measurements and physical parameter inversion. The two modules operate in synergy, enabling a paradigm shift from "scheduled acquisition, post-processing" to "event-driven, real-time response, intelligent autonomous" observations.

YOGIS requires not only technological upgrades but also sustained advancements in scientific frontiers and application extensions. Single-platform, single-wavelength observations are inherently insufficient to simultaneously disentangle the complex coupling among the coronal magnetic field, velocity field, and temperature field. There is an urgent need to develop a synergistic ground-based and space-borne, multi-perspective, multi-wavelength joint detection system. In this context, collaborative observations integrating international forefront solar facilities—such as the Daniel K. Inouye Solar Telescope (DKIST), the SDO/AIA, and the Upgraded Coronal Multi-channel Polarimeter (UCoMP)—are imperative. Addressing the challenge of coronal magnetometry through synergistic observations, constructing an integrated space–ground detection network with homegrown instruments, empowering precise CME forecasting with artificial intelligence, and leading international cooperation via data sharing—these four mutually reinforcing and progressively advancing directions collectively define the contemporary frontier of coronal physics and space weather science.

 doi:10.20944/preprints202602.1308.v1

Author Contributions: Conceptualization, X.Z. and Y.L.; methodology, X.Z., T.S., and M.S.; software, M.Z.; investigation, X.L.; data curation, F.S. and X.L.; writing—original draft preparation, X.Z.; writing—review and editing, X.Z. and Y.L.; funding acquisition, Y.L. All authors have read and agreed to the published version of the manuscript.

Funding: This work was jointly supported by multiple funding sources. Specifically, it received partial support from the National Natural Science Foundation of China (NSFC grant Nos. 12173086, 12373063, 11533009, 12163004, 12473089, and 42274227). Additionally, the Yunnan Fundamental Research Projects (grant Nos. 202501AS070004 and 202401AT070140), and the Yunnan Key Laboratory of Solar Physics and Space Science (grant No. 202205AG070009).

Data Availability Statement: Data are contained within the article.

Acknowledgments: We sincerely thank the NAOJ team for the long-term 10 cm coronagraph collaborations, and acknowledge the data resources from the National Space Science Data Center, National Science and Technology Infrastructure of China (http://www.nssdc.ac.cn). We acknowledge the Chinese Meridian Project for providing high-quality data from the SICG. We also thank the NASA/SDO and the AIA science team for open data access. We thank the anonymous referees for helpful comments and suggestions on the manuscript.

Conflicts of Interest: The authors declare no conflicts of interest.

References

1. Wang, Y.M.; Sheeley, Jr., N.R.; Hawley, S.H.; Kraemer, J.R.; Brueckner, G.E.; Howard, R.A.; Korendyke, C.M.; Michels, D.J.; Moulton, N.E.; Socker, D.G.; et al. The Green Line Corona and Its Relation to the Photospheric Magnetic Field. *ApJ* **1997**, *485*, 419–429. https://doi.org/10.1086/304405.
2. Yang, Z.; Tian, H.; Tomczyk, S.; Liu, X.; Gibson, S.; Morton, R.J.; Downs, C. Observing the evolution of the Sun's global coronal magnetic field over 8 months. *Science* **2024**, *386*, 76–82, [arXiv:astro-ph.SR/2410.16555]. https://doi.org/10.1126/science.ado2993.
3. Chen, Y.; Bai, X.; Tian, H.; Li, W.; Chen, F.; Yang, Z.; Yang, Y. Solar coronal magnetic field measurements using spectral lines available in Hinode/EIS observations: strong and weak field techniques and temperature diagnostics. *MNRAS* **2023**, *521*, 1479–1488, [arXiv:astro-ph.SR/2302.10596]. https://doi.org/10.1093/mnras/stad583.
4. Song, H.; Wang, R.; Li, L.; Wang, B.; Chen, Y. On the Nature of the Bright Front of Solar Coronal Mass Ejections. *ApJ* **2025**, *988*, 270. https://doi.org/10.3847/1538-4357/adec88.
5. Lyot, B. The study of the solar corona and prominences without eclipses (George Darwin Lecture, 1939). *MNRAS* **1939**, *99*, 580. https://doi.org/10.1093/mnras/99.8.580.
6. Tian, H.; Tomczyk, S.; McIntosh, S.W.; Bethge, C.; de Toma, G.; Gibson, S. Observations of Coronal Mass Ejections with the Coronal Multichannel Polarimeter. *Sol. Phys.* **2013**, *288*, 637–650, [arXiv:astro-ph.SR/1303.4647]. https://doi.org/10.1007/s11207-013-0317-5.
7. de Wijn, A.G.; Burkepile, J.T.; Tomczyk, S.; Nelson, P.G.; Huang, P.; Gallagher, D. Stray light and polarimetry considerations for the COSMO K-Coronagraph. In Proceedings of the Ground-based and Airborne Telescopes IV; Stepp, L.M.; Gilmozzi, R.; Hall, H.J., Eds., September 2012, Vol. 8444, *Society of Photo-Optical Instrumentation Engineers (SPIE) Conference Series*, p. 84443N, [arXiv:astro-ph.IM/1207.0978]. https://doi.org/10.1117/12.926511.
8. Han, Y.; Yang, Q.; Liu, N.; Zhang, K.; Qing, C.; Li, X.; Wu, X.; Luo, T. Analysis of wind-speed profiles and optical turbulence above Gaomeigu and the Tibetan Plateau using ERA5 data. *MNRAS* **2021**, *501*, 4692–4702. https://doi.org/10.1093/mnras/staa2960.
9. Rao, C.; Zhu, L.; Rao, X.; Zhang, L.; Bao, H.; Kong, L.; Guo, Y.; Zhong, L.; Ma, X.; Li, M.; et al. Instrument Description and Performance Evaluation of a High-Order Adaptive Optics System for the 1 m New Vacuum Solar Telescope at Fuxian Solar Observatory. *ApJ* **2016**, *833*, 210. https://doi.org/10.3847/1538-4357/833/2/210.
10. Ichimoto, K.; Noguchi, M.; Tanaka, N.; Kumagai, K.; Shinoda, K.; Nishino, T.; Fukuda, T.; Sakurai, T.; Takeyama, N. A New Imaging System of the Corona at Norikura. *PASJ* **1999**, *51*, 383–391. https://doi.org/10.1093/pasj/51.3.383.
11. Sakurai, T. Sixty Years of Norikura Solar Observatory. In Proceedings of the Hinode-3: The 3rd Hinode Science Meeting; Sekii, T.; Watanabe, T.; Sakurai, T., Eds., August 2012, Vol. 454, *Astronomical Society of the Pacific Conference Series*, p. 439.

 doi:10.20944/preprints202602.1308.v1

12. Song, T.; Liu, Y.; Zhang, X.; Zhao, M.; Li, X.; Luo, Q.; Sha, F.; Liu, Q.; Oloketuyi, J.; Wang, X. Toward Automated Coronal Observations: A New Integrated System Based on the Lijiang 10 cm Coronagraph. *Universe* **2025**, *11*, 154. https://doi.org/10.3390/universe11050154.
13. Xu, J.; Feng, G.j.; Pu, G.x.; Wang, L.t.; Cao, Z.H.; Ren, L.Q.; Zhang, X.; Ma, S.g.; Bai, C.h.; Esamdin, A.; et al. Site-testing at the Muztagh-ata Site V. Nighttime Cloud Amount during the Last Five Years. *Research in Astronomy and Astrophysics* **2023**, *23*, 045015, [arXiv:astro-ph.IM/2305.03067]. https://doi.org/10.1088/1674-4527/acc29b.
14. Lemen, J.R.; Title, A.M.; Akin, D.J.; Boerner, P.F.; Chou, C.; Drake, J.F.; Duncan, D.W.; Edwards, C.G.; Friedlaender, F.M.; Heyman, G.F.; et al. The Atmospheric Imaging Assembly (AIA) on the Solar Dynamics Observatory (SDO). *Sol. Phys.* **2012**, *275*, 17–40. https://doi.org/10.1007/s11207-011-9776-8.
15. Liu, Y.; Zhang, X.; Song, T.; Sun, M.; Liu, D.; Wang, J.; Zhao, M.; Zhang, T.; Xu, F.; Fu, H.; et al. Ground experiment of a 50 mm balloon-borne coronagraph for near space project. In Proceedings of the 10th International Symposium on Advanced Optical Manufacturing and Testing Technologies: Large Mirror and Telescopes; Rao, C.H.; Veillet, C.; Ma, X.; Fan, B.; Liu, F.; Collados Vera, M., Eds., December 2021, Vol. 12070, *Society of Photo-Optical Instrumentation Engineers (SPIE) Conference Series*, p. 120700B. https://doi.org/10.1117/12.2605310.
16. Li, Y.; Huang, W.; Zhou, J.; Zhang, X.; Zhang, H. Development Status and Prospects of Near Space Observatories. *Chinese Journal of Space Science* **2024**, *44*, 1068–1085. https://doi.org/10.11728/cjss2024.06.2023-0145.
17. Gopalswamy, N.; Newmark, J.; Yashiro, S.; Mäkelä, P.; Reginald, N.; Thakur, N.; Gong, Q.; Kim, Y.H.; Cho, K.S.; Choi, S.H.; et al. The Balloon-Borne Investigation of Temperature and Speed of Electrons in the Corona (BITSE): Mission Description and Preliminary Results. *Sol. Phys.* **2021**, *296*, 15, [arXiv:astro-ph.SR/2011.06111]. https://doi.org/10.1007/s11207-020-01751-8.
18. Song, H.; Li, L.; Zhou, Z.; Xia, L.; Cheng, X.; Chen, Y. The Structure of Coronal Mass Ejections Recorded by the K-Coronagraph at Mauna Loa Solar Observatory. *ApJ Lett.* **2023**, *952*, L22, [arXiv:astro-ph.SR/2307.01398]. https://doi.org/10.3847/2041-8213/ace422.
19. Tan, H.; Cen, X.F.; Qian, T.L.; Wang, J.C. Evaluation of Lijiang Gaomeigu site for astrophysical observation. *Bulletin of the Astronomical Society of India* **2002**, *30*, 881–893.
20. ASCOM Initiative. ASCOM Standards. https://www.ascom-standards.org, 2025. Accessed: 2025-12-30.
21. Sha, F.; Liu, Y.; Zhang, X.; Song, T. Characterization and Correction of the Scattering Background Produced by Dust on the Objective Lens of the Lijiang 10-cm Coronagraph. *Sol. Phys.* **2023**, *298*, 139, [arXiv:astro-ph.IM/2311.14784]. https://doi.org/10.1007/s11207-023-02233-3.
22. Sha, F.; Liu, Y.; Xia, L.; Chen, Y.; Zhou, Q.; Chen, Y.; Zhong, C.; Zhang, X.; Song, T.; Sun, M.; et al. Mapping Ground-based Coronagraphic Images to Helioprojective-Cartesian Coordinate System by Image Registration. *ApJ* **2025**, *990*, 56, [arXiv:astro-ph.SR/2507.17670]. https://doi.org/10.3847/1538-4357/adf05e.
23. Zhang, X.F.; Liu, Y.; Zhao, M.Y.; Song, T.F.; Wang, J.X.; Li, X.B.; Li, Z.H. On the Relation Between Coronal Green Line Brightness and Magnetic Fields Intensity. *Research in Astronomy and Astrophysics* **2022**, *22*, 075007. https://doi.org/10.1088/1674-4527/ac6fb8.
24. Zhang, X.F.; Liu, Y.; Zhao, M.Y.; Liu, J.H.; Elmhamdi, A.; Song, T.F.; Li, Z.H.; Li, H.B.; Sha, F.Y.; Wang, J.X.; et al. Comparison of the Coronal Green-line Intensities with the EUV Measurements from SDO/AIA. *Research in Astronomy and Astrophysics* **2022**, *22*, 075012. https://doi.org/10.1088/1674-4527/ac712e.
25. Woods, T.N.; Eden, T.; Eparvier, F.G.; Jones, A.R.; Woodraska, D.L.; Chamberlin, P.C.; Machol, J.L. GOES-R Series X-Ray Sensor (XRS): 1. Design and Pre-Flight Calibration. *Journal of Geophysical Research (Space Physics)* **2024**, *129*, 2024JA032925. https://doi.org/10.1029/2024JA032925.
26. De Moortel, I.; Browning, P. Recent advances in coronal heating. *Philosophical Transactions of the Royal Society of London Series A* **2015**, *373*, 20140269–20140269, [arXiv:astro-ph.SR/1510.00977]. https://doi.org/10.1098/rsta.2014.0269.
27. Mason, J.P.; Werth, A.; West, C.G.; Youngblood, A.; Woodraska, D.L.; Peck, C.L.; Aradhya, A.J.; Cai, Y.; Chaparro, D.; Erikson, J.W.; et al. Coronal Heating as Determined by the Solar Flare Frequency Distribution Obtained by Aggregating Case Studies. *ApJ* **2023**, *948*, 71, [arXiv:astro-ph.SR/2305.05687]. https://doi.org/10.3847/1538-4357/accc89.
28. Yang, K.E.; Longcope, D.W.; Ding, M.D.; Guo, Y. Observationally quantified reconnection providing a viable mechanism for active region coronal heating. *Nature Communications* **2018**, *9*, 692, [arXiv:astro-ph.SR/1802.06206]. https://doi.org/10.1038/s41467-018-03056-8.

 doi:10.20944/preprints202602.1308.v1

29. Badalyan, O.G.; Beigman, I.L.; Livshits, M.A. Polarization of the Solar Corona in the Green Line: Contradiction Between Theory and Observations. *Astronomy Reports* **2001**, *45*, 321–329. https://doi.org/10.1134/1.1361325.
30. Badalyan, O.G.; Livshits, M.A.; Sýkora, J. Relationship between polarization and intensity of the green line in different coronal structures. *A&A* **1999**, *349*, 295–300.
31. Judge, P.G.; Habbal, S.; Landi, E. From Forbidden Coronal Lines to Meaningful Coronal Magnetic Fields. *Sol. Phys.* **2013**, *288*, 467–480, [arXiv:astro-ph.SR/1304.3863]. https://doi.org/10.1007/s11207-013-0309-5.